



# Solid-Liquid Equilibrium Calculation and Parameters Determination in Thermodynamic Models for Binary and Ternary Fatty Mixtures

Stella A. Rocha<sup>a</sup>, Lincoln K. da Silva<sup>a</sup>, Laslo A. D. Boros<sup>b</sup>,

Maria A. Krahenbuhl<sup>b</sup>, Reginaldo Guirardello<sup>b</sup>

<sup>a</sup>Department of Chemistry, IFPR - Federal Institute of Paraná – Campus Umuarama Road PR 323, s/n, CEP 87507-014, Umuarama - PR, Brazil.

<sup>b</sup>School of Chemical Engineering, University of Campinas - UNICAMP, Av. Albert Einstein 500, CEP 13083-852, Campinas - SP, Brazil.  
 stella.rocha@ifpr.edu.br

This work has a theoretical and computational character, whose objective is the study and application of an optimization technique for the solid-liquid equilibrium calculation. Focused on binary and ternary fatty mixtures with natural origin, this work can also be applied for different mixtures of fatty acids, triglycerides and ethyl esters using the minimization of Gibbs Energy of the systems. This problem was formulated as a non-linear program, and convexity analysis ensured that the optimal solution found was the global optimum. The equilibrium problem was implemented in software GAMS in addition of Microsoft Excel, where the description of phases was done based on two thermodynamic models. The solid phase was characterized using a modified Slaughter and Doherty model, while the liquid phase was modeled with Margules 2 – suffixes and the Wilson Model. In the liquid phase, the Margules model assumes two forms: Margules Asymmetric, where the Margules parameters are different, and Margules Symmetric, with equal Margules parameters. In this work specifically, it was calculated the equilibrium points with some combinations of myristic, palmitic and capric acids; ethyl laurate, miristate and palmitate; tripalmitin and tristearin was calculated. Experimental data was used in comparative mode of binary mixtures, with good agreement between experimental and calculated points; new equilibrium data were predicted and obtained for ternary mixtures, and the parameters model also was determined. The results were described in the form of phase diagrams for binary mixtures and surfaces of equilibrium for ternary mixtures, where the equilibrium data and the parameters model were calculated based on the square errors, and fitted well to the experimental data.

## 1. Introduction

The prediction of solid-liquid equilibrium is important to describe the phase formation and the compositions of many chemical processes. The separation processes, which need the solid-liquid phase data, have been studied for many years, but now, with high and newer technological developments, the theoretical and practical interest in this area has increased (Rocha and Guirardello, 2009). Mainly focused on fatty mixtures, the solid-liquid equilibrium is essential for biofuel separation process. So, it is necessary the improvement of the thermodynamic models capable of precisely representing the equilibrium (Rangaiah, 2001).

The correct determination of phase formation is indispensable for prediction of solid-liquid equilibrium, specifically because of important points, like eutectic and peritectic points, so that thermodynamic models need to be capable to represent, and more than this, need to identify when this behavior is present (Inoue et al, 2004).

The solid-liquid equilibrium can be calculated in many ways. In the present work, the minimization of the Gibbs free energy was chosen as a starting point to calculate the equilibrium. This technique is considered sufficient to guarantee finding the equilibrium point, if the global minimum is found (Smith et al, 2004).

The general approach in this work applies the same assumptions used by Slaughter and Doherty (Slaughter and Doherty, 1995), but the approach used here leads to an easier way to calculate the temperature profiles, with explicit expressions. The thermodynamic representation of the solid and liquid phases was done using specific models for each phase. The solid phase was modeled using a modification of the activity model described by Slaughter and Doherty (Slaughter and Doherty, 1995), using a mathematical limit (Rocha and Guirardello, 2009). The liquid phase was modeled using Margules 2-suffix equation, in the symmetric and asymmetric form, and Wilson, but the approach is easily generalized to other models for the liquid phase. The equations obtained resulted in an expression for the Gibbs free energy. The phases diagrams had been formed by the application of the Kuhn-Tucker condition and convexity analysis (Rocha and Guirardello, 2009). This method was applied for binary and ternary mixtures, with different combination of fatty acids, triglycerides and ethyl ester.

## 2. Thermodynamic Model

The thermodynamic analysis showed three possible equilibrium regions. These regions are related with the characteristic form of the phase diagrams, where region 1 is represented by liquidus line, which begins in molar fraction equal 0 ( $x_A = 0$ ) until peritectic point; region 2, named solidus line, in the sequence of graphics is located since eutectic point until the maximum molar fraction; and region 3 is the interval between the peritectic and eutectic points, if this region exists.

The mathematical models used in this work can be divided according the sub items described below. This classification follows the proposed idea to calculate the equilibrium using the mathematical thermodynamic model development to found the equilibrium points for binary and ternary mixtures. Based on equations already demonstrated by Rocha and Guirardello (2009), for all models, some basic conditions are described below, by Eqs (1), (2), (3), (4), (5) and (6):

- region I:

$$T(x_1 = 1) = 0 \quad (1)$$

- region II:

$$T(x_1 = 0) = 0 \quad (2)$$

- region III:

$$T(x_1 = 0) = 0 \quad (3)$$

$$T(x_1 = 1) = 0 \quad (4)$$

$$\frac{dT}{dx_1} = 0 \quad \text{with} \quad x_1 = x_{1C} \quad (5)$$

$$x_{1C} = \frac{V_1}{V_1 + V_2} \quad (6)$$

where  $V_i$  represents the stoichiometric coefficients and  $x_{1C}$  represents the molar fraction where the intermediate solid compound occurs (peritectic point).

The equilibrium temperature can then be calculated by Eq (7), for each given molar fraction,  $X_1$  and  $X_2$ :

$$T = \max \{T_I, T_{II}, T_{III}\} \quad (7)$$

## 3. Phase Diagrams for Solid-Liquid Equilibrium

By applying the condition of minimum  $G$  in the number of moles, at constant  $T$  and  $P$ , the phases diagrams were obtained for three different models for binary mixtures and two models for ternary mixtures, based on the division of the phases diagram in three regions, as previously described.

### 3.1 Margules Asymmetric – Binary Mixtures

From the Margules Model, the excess  $G$  given by Eq (8), and its activity coefficients, Eqs (9) and (10), the solid-liquid equilibrium can be represented by regions 1, Eq (11), region 2, Eq (12) and region 3, Eq (13).

$$\underline{G}_{\text{ex}}^l = R \cdot T \cdot \sum_{i=1}^{NC} x_i^l \cdot \ln \gamma_i^l = x_1^l \cdot x_2^l \cdot (A_{21} \cdot x_1^l + A_{12} \cdot x_2^l) \quad (8)$$

$$R \cdot T \cdot \ln \gamma_1 = [A_{12} + 2 \cdot (A_{21} - A_{12}) \cdot x_1] \cdot x_2^2 \quad (9)$$

$$R \cdot T \cdot \ln \gamma_2 = [A_{21} + 2 \cdot (A_{12} - A_{21}) \cdot x_2] \cdot x_2^2 \quad (10)$$

$$T_I = \frac{\Delta h_{f2} + [A_{21} + 2 \cdot (A_{12} - A_{21}) \cdot (1 - x_1)] \cdot x_1^2}{\frac{\Delta h_{f2}}{T_{f2}} - R \cdot \ln(1 - x_1)} \quad (11)$$

$$T_{II} = \frac{\Delta h_{f1} + [A_{12} + 2 \cdot (A_{21} - A_{12}) \cdot x_1] \cdot (1 - x_1)^2}{\frac{\Delta h_{f1}}{T_{f1}} - R \cdot \ln x_1} \quad (12)$$

$$T_{III} = \frac{v_1 \cdot \Delta h_{f1} + v_2 \cdot \Delta h_{f2} + v_1 \cdot [A_{12} + 2 \cdot (A_{21} - A_{12}) \cdot x_1] \cdot (1 - x_1)^2 + v_2 \cdot [A_{21} + 2 \cdot (A_{12} - A_{21}) \cdot (1 - x_1)] \cdot x_1^2 + \Delta G_R^\circ}{v_1 \cdot \frac{\Delta h_{f1}}{T_{f1}} + v_2 \cdot \frac{\Delta h_{f2}}{T_{f2}} - v_1 \cdot R \cdot \ln x_1 - v_2 \cdot R \cdot \ln(1 - x_1)} \quad (13)$$

subject to restriction (14):

$$\frac{\Delta h_{f2} + [A_{21} + 2 \cdot (A_{12} - A_{21}) \cdot (1 - x_{1C})] \cdot x_{1C}^2}{\frac{\Delta h_{f2}}{T_{f2}} - R \cdot \ln(1 - x_{1C})} \leq \frac{\Delta h_{f1} + [A_{12} + 2 \cdot (A_{21} - A_{12}) \cdot x_{1C}] \cdot (1 - x_{1C})^2 + \frac{1}{v_1} \cdot \Delta G_R^\circ}{\frac{\Delta h_{f1}}{T_{f1}} - R \cdot \ln x_{1C}} \quad (14)$$

### 3.2 Margules Symmetric – Binary Mixtures

Using Margules Model in the form described in Eq (15), for the excess G, the binaries interaction parameters, considering constant temperature, could be described by Eq (16).

$$G_{\text{ex}}^I = R \cdot T \cdot \sum_{i=1}^{NC} x_i^I \cdot \ln \gamma_i^I = \frac{1}{2} \cdot \sum_{i=1}^{NC} \sum_{j=1}^{NC} A_{ij} \cdot x_i^I \cdot x_j^I \quad (15)$$

$$A_{ji} = A_{ij} = a_{ij} \quad (16)$$

The definition of regions 1, 2 and 3 are, respectively, showed by Eqs (17), (18) and (19):

$$T_I = \frac{\Delta h_{f2} + a_{12} \cdot x_1^2}{\frac{\Delta h_{f2}}{T_{f2}} - R \cdot \ln(1 - x_1)} \quad (17)$$

$$T_{II} = \frac{\Delta h_{f1} + a_{12} \cdot (1 - x_1)^2}{\frac{\Delta h_{f1}}{T_{f1}} - R \cdot \ln x_1} \quad (18)$$

$$T_{III} = \frac{v_1 \cdot \Delta h_{f1} + v_2 \cdot \Delta h_{f2} + v_1 \cdot a_{12} \cdot (1 - x_1)^2 + v_2 \cdot a_{12} \cdot x_1^2 + \Delta G_R^\circ}{v_1 \cdot \frac{\Delta h_{f1}}{T_{f1}} + v_2 \cdot \frac{\Delta h_{f2}}{T_{f2}} - v_1 \cdot R \cdot \ln x_1 - v_2 \cdot R \cdot \ln(1 - x_1)} \quad (19)$$

subject to restriction (20):

$$\frac{\Delta h_{f2} + a_{12} \cdot x_{1C}^2}{\frac{\Delta h_{f2}}{T_{f2}} - R \cdot \ln(1 - x_{1C})} \leq \frac{\Delta h_{f1} + a_{12} \cdot (1 - x_{1C})^2 + \frac{1}{v_1} \cdot \Delta G_R^\circ}{\frac{\Delta h_{f1}}{T_{f1}} - R \cdot \ln x_{1C}} \quad (20)$$

### 3.3 Wilson – Binary Mixtures

The Wilson model has their activity coefficients showed by Eqs (21) and (22):

$$\ln \gamma_1 = -\ln(x_1 + x_2 \Lambda_{12}) + x_2 \left( \frac{\Lambda_{12}}{x_1 + x_2 \Lambda_{12}} - \frac{\Lambda_{21}}{x_2 + x_1 \Lambda_{21}} \right) \quad (21)$$

$$\ln \gamma_2 = -\ln(x_2 + x_1 \Lambda_{21}) + x_1 \left( \frac{\Lambda_{12}}{x_1 + x_2 \Lambda_{12}} - \frac{\Lambda_{21}}{x_2 + x_1 \Lambda_{21}} \right) \quad (22)$$

The region's equations that describe the equilibrium curves are Eqs (23), (24) and (25):

$$T_I = \frac{\Delta h_{f2}}{\frac{\Delta h_{f2}}{T_{f2}} - R \cdot \left( \ln(1-x_1) - \ln((1-x_1) + x_1 \Lambda_{21}) + x_1 \left( \frac{\Lambda_{12}}{x_1 + (1-x_1)\Lambda_{12}} - \frac{\Lambda_{21}}{(1-x_1) + x_1 \Lambda_{21}} \right) \right)} \quad (23)$$

$$T_{II} = \frac{\Delta h_{f1}}{\frac{\Delta h_{f1}}{T_{f1}} - R \cdot \left( \ln x_1 - \ln(x_1 + (1-x_1)\Lambda_{12}) + (1-x_1) \cdot \left( \frac{\Lambda_{12}}{x_1 + (1-x_1)\Lambda_{12}} - \frac{\Lambda_{21}}{(1-x_1) + x_1 \Lambda_{21}} \right) \right)} \quad (24)$$

$$T_{III} = \frac{v_1 \cdot \Delta h_{f1} + v_2 \cdot \Delta h_{f2} + \Delta G_R^\circ}{v_1 \cdot \frac{\Delta h_{f1}}{T_{f1}} - v_1 \cdot R \cdot \left( \ln x_1 - \ln(x_1 + (1-x_1)\Lambda_{12}) + (1-x_1) \cdot \left( \frac{\Lambda_{12}}{x_1 + (1-x_1)\Lambda_{12}} - \frac{\Lambda_{21}}{(1-x_1) + x_1 \Lambda_{21}} \right) \right)} \quad (25)$$

$$+ \frac{v_1 \cdot \Delta h_{f1} + v_2 \cdot \Delta h_{f2} + \Delta G_R^\circ}{v_2 \cdot \frac{\Delta h_{f2}}{T_{f2}} - v_2 \cdot R \cdot \left( \ln(1-x_1) - \ln((1-x_1) + x_1 \Lambda_{21}) + x_1 \left( \frac{\Lambda_{12}}{x_1 + (1-x_1)\Lambda_{12}} - \frac{\Lambda_{21}}{(1-x_1) + x_1 \Lambda_{21}} \right) \right)}$$

subject to restriction (26):

$$\frac{\frac{\Delta h_{f2}}{T_{f2}} - R \cdot \left( \ln(1-x_{1C}) - \ln((1-x_{1C}) + x_{1C}\Lambda_{21}) + x_{1C} \left( \frac{\Lambda_{12}}{x_{1C} + (1-x_{1C})\Lambda_{12}} - \frac{\Lambda_{21}}{(1-x_{1C}) + x_{1C}\Lambda_{21}} \right) \right)}{\frac{\Delta h_{f1}}{T_{f1}} - R \cdot \left( \ln x_{1C} - \ln(x_{1C} + (1-x_{1C})\Lambda_{12}) + (1-x_{1C}) \cdot \left( \frac{\Lambda_{12}}{x_{1C} + (1-x_{1C})\Lambda_{12}} - \frac{\Lambda_{21}}{(1-x_{1C}) + x_{1C}\Lambda_{21}} \right) \right)} \leq \frac{\Delta h_{f1} + \frac{1}{v_1} \cdot \Delta G_R^\circ}{\frac{\Delta h_{f1}}{T_{f1}} - R \cdot \left( \ln x_{1C} - \ln(x_{1C} + (1-x_{1C})\Lambda_{12}) + (1-x_{1C}) \cdot \left( \frac{\Lambda_{12}}{x_{1C} + (1-x_{1C})\Lambda_{12}} - \frac{\Lambda_{21}}{(1-x_{1C}) + x_{1C}\Lambda_{21}} \right) \right)} \quad (26)$$

### 3.4 Margules Asymmetric – Ternary Mixtures

This model was based on solidification temperature in solid-liquid equilibrium for ternary mixtures. Considering three compounds ( $A_1, A_2, A_3$ ) and the intermediate solid compound (peritectic point) formed only by two of them, where the solidification temperature was set as the maximum temperature of each composition. The Margules Asymmetric model leads to Eq (27) for  $T$ , and Eq (28) for the peritectic region.

$$T_i = \frac{\Delta h_i^f + c_i}{\frac{\Delta h_i^f}{T_i^f} - R \cdot \ln x_i} \quad i = 1, 2, 3 \quad (27)$$

$$T_p = \frac{v_1 \cdot \Delta h_{f1} + v_2 \cdot \Delta h_{f2} + v_1 \cdot c_1 + v_2 \cdot c_2 + \Delta G_R^\circ}{v_1 \cdot \frac{\Delta h_{f1}}{T_{f1}} + v_2 \cdot \frac{\Delta h_{f2}}{T_{f2}} - v_1 \cdot R \cdot \ln x_1 - v_2 \cdot R \cdot \ln x_2} \quad (28)$$

where:

$$\begin{aligned} c_1 &= A_{12} \cdot x_2^2 \cdot (1-2 \cdot x_1) + 2 \cdot A_{21} \cdot x_1 \cdot x_2 \cdot (1-x_1) + A_{13} \cdot x_3^2 \cdot (1-2 \cdot x_1) + 2 \cdot A_{31} \cdot x_1 \cdot x_3 \cdot (1-x_1) \\ &\quad - 2 \cdot A_{23} \cdot x_2 \cdot x_3^2 - 2 \cdot A_{32} \cdot x_2^2 \cdot x_3 + \left[ \frac{1}{2} \cdot (A_{12} + A_{21} + A_{13} + A_{31} + A_{23} + A_{32}) - Q \right] \cdot (x_2 \cdot x_3 - 2 \cdot x_1 \cdot x_2 \cdot x_3) \\ c_2 &= A_{21} \cdot x_1^2 \cdot (1-2 \cdot x_2) + 2 \cdot A_{12} \cdot x_1 \cdot x_2 \cdot (1-x_2) + A_{23} \cdot x_3^2 \cdot (1-2 \cdot x_2) + 2 \cdot A_{32} \cdot x_2 \cdot x_3 \cdot (1-x_2) \\ &\quad - 2 \cdot A_{13} \cdot x_1 \cdot x_3^2 - 2 \cdot A_{31} \cdot x_1^2 \cdot x_3 + \left[ \frac{1}{2} \cdot (A_{12} + A_{21} + A_{13} + A_{31} + A_{23} + A_{32}) - Q \right] \cdot (x_1 \cdot x_3 - 2 \cdot x_1 \cdot x_2 \cdot x_3) \\ c_3 &= A_{31} \cdot x_1^2 \cdot (1-2 \cdot x_3) + 2 \cdot A_{13} \cdot x_1 \cdot x_3 \cdot (1-x_3) + A_{32} \cdot x_2^2 \cdot (1-2 \cdot x_3) + 2 \cdot A_{23} \cdot x_2 \cdot x_3 \cdot (1-x_3) \\ &\quad - 2 \cdot A_{12} \cdot x_1 \cdot x_2^2 - 2 \cdot A_{21} \cdot x_1^2 \cdot x_2 + \left[ \frac{1}{2} \cdot (A_{12} + A_{21} + A_{13} + A_{31} + A_{23} + A_{32}) - Q \right] \cdot (x_1 \cdot x_2 - 2 \cdot x_1 \cdot x_2 \cdot x_3) \end{aligned}$$

with  $Q = 0$  in this work.

### 3.5 Wilson – Ternary Mixtures

In the same way of Margules model, the Wilson model resulted in Eqs (29) and (30) for  $T$ .

$$T_i = \frac{\Delta h_i^f}{\frac{\Delta h_i^f}{T_i^f} - R \cdot [\ln x_i + \ln \gamma_i]} \quad i = 1,2,3 \quad (29)$$

$$T_p = \frac{v_1 \cdot \Delta h_{f1} + v_2 \cdot \Delta h_{f2} + \Delta G_R^0}{v_1 \cdot \frac{\Delta h_{f1}}{T_{f1}} + v_2 \cdot \frac{\Delta h_{f2}}{T_{f2}} - v_1 \cdot R \cdot [\ln x_1 + \ln \gamma_1] - v_2 \cdot R \cdot [\ln x_2 + \ln \gamma_2]} \quad (30)$$

where the activity coefficients are described by Eqs (31), (32) and (33):

$$\ln \gamma_1 = 1 - \ln(x_1 + x_2 \Lambda_{12} + x_3 \Lambda_{13}) - \left( \frac{x_1}{x_1 + x_2 \Lambda_{12} + x_3 \Lambda_{13}} + \frac{x_2 \Lambda_{21}}{x_1 \Lambda_{21} + x_2 + x_3 \Lambda_{23}} + \frac{x_3 \Lambda_{31}}{x_1 \Lambda_{31} + x_2 \Lambda_{32} + x_3} \right) \quad (31)$$

$$\ln \gamma_2 = 1 - \ln(x_1 \Lambda_{21} + x_2 + x_3 \Lambda_{23}) - \left( \frac{x_1 \Lambda_{12}}{x_1 + x_2 \Lambda_{12} + x_3 \Lambda_{13}} + \frac{x_2}{x_1 \Lambda_{21} + x_2 + x_3 \Lambda_{23}} + \frac{x_3 \Lambda_{32}}{x_1 \Lambda_{31} + x_2 \Lambda_{32} + x_3} \right) \quad (32)$$

$$\ln \gamma_3 = 1 - \ln(x_1 \Lambda_{31} + x_2 \Lambda_{32} + x_3) - \left( \frac{x_1 \Lambda_{13}}{x_1 + x_2 \Lambda_{12} + x_3 \Lambda_{13}} + \frac{x_2 \Lambda_{23}}{x_1 \Lambda_{21} + x_2 + x_3 \Lambda_{23}} + \frac{x_3}{x_1 \Lambda_{31} + x_2 \Lambda_{32} + x_3} \right) \quad (33)$$

#### 4. Results of Case Studies

In this section, some binary and ternary mixtures are considered as case studies. Four binary mixtures are considered: ethyl laurate (1) – ethyl palmitate (2), ethyl laurate (1) – ethyl miristate (2), myristic acid (1) – palmitic acid (2) and tripalmitin (1) – tristearin; and the results are demonstrated by phases diagrams, in Figure 1 a-d. The ternary mixture is ethyl laurate (1) – ethyl miristate (2) – ethyl palmitate (3), and the result is a equilibrium surface (Figure 2).

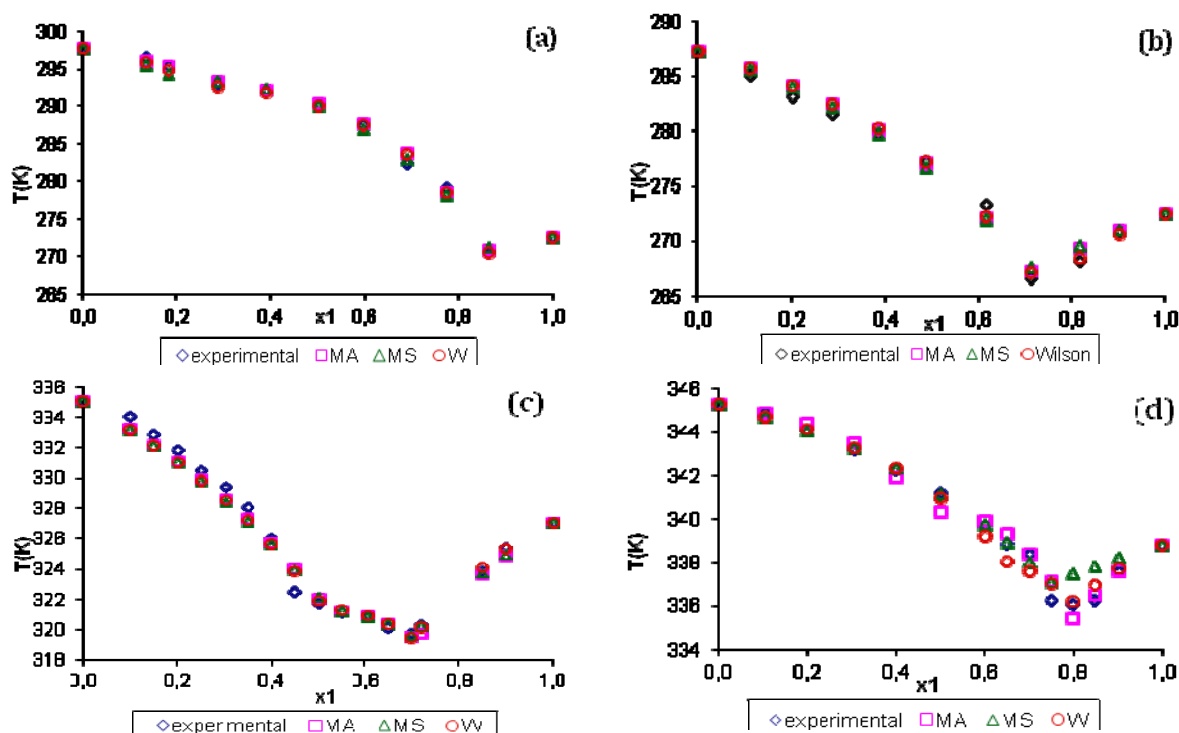


Figure 1: Solid-liquid equilibrium diagram for ethyl laurate (1) – ethyl palmitate (2) (a); ethyl laurate (1) – ethyl miristate (2)(b); myristic acid (1) – palmitic acid (2) (c) and ethyl tripalmitin (1) – tristearin (2)(d).

The methodology was based on calculated solid-liquid phases diagram, with or without the formation of intermediate solid compounds, by the minimization of Gibbs free energy using the thermodynamic models already described. The curve fitting was done by the sum of squared errors, using the software GAMS, where the calculated temperatures were compared with experimental ones obtained by DSC technique.

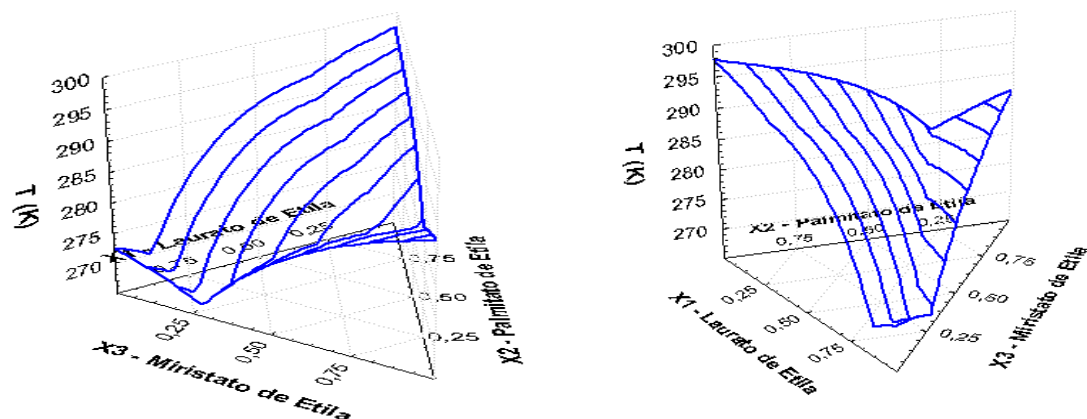


Figure 2: Two visions of the solid-liquid equilibrium surface for ethyl laurate (1) – ethyl miristate (2) – ethyl palmitate (3).

## 5. Conclusions

In this work, equations for the temperature as a function of molar fraction were used to calculate the phase diagram for solid–liquid equilibrium, including the presence of both peritectic and eutectic points. The models developed showed to be easy and efficient in describing phenomenon on the liquidus line by both the Margules models and Wilson model. The ternary surface showed the applicability and diverse possibilities for composition of oils and fatties. Five case studies were considered to demonstrate the methodology, which was very easy to apply. The results were satisfactory, in good agreement with experimental data, for all mixtures studied in this work, which have strong interest for the biofuel industry.

## References

- Boros L., Batista M.L.S., Vaz R.V., Figueiredo B.R., Fernandes V.F.S., Costa M.C., Krähenbühl M.A., Meirelles A.J.A., Coutinho J.A.P., 2009, Crystallization Behavior of Mixtures of Fatty Acid Ethyl Esters with Ethyl Stearate. *Energy Fuel*, 23, 4625-4629.
- Costa M.C., Sardob M., Rolemberg M.P., Coutinho J.A.P., Meirelles A.J.A., Ribeiro-Claro P., Krähenbühl M.A., 2009, The solid–liquid phase diagrams of binary mixtures of consecutive, even saturated fatty acids, *Chemistry and Physics of Lipids* 160, pp. 85-97.
- Costa M.C., Boros L., Batista M.L.S., Coutinho J.A.P., Krähenbühl M.A., Meirelles A.J.A., 2010 a, Phase diagrams of mixtures of ethyl palmitate with fatty acid ethyl esters. *Fuel Process. Technol.*
- Costa M.C., Boros L.A.D., Coutinho J.A.P., Krähenbühl M.A., Meirelles A.J.A., 2010 b, Low temperature behavior of biodiesel: Solid-liquid phase diagrams of binary mixtures composed of fatty acid methyl esters. *Fuel*.
- Inoue T., Hisatsugua Y., Suzukib M., Wangc Z., Zheng L., Solid–liquid phase behavior of binary fatty acid mixtures 3. 2004, Mixtures of oleic acid with capric acid (decanoic acid) and caprylic acid (octanoic acid) *Chemistry and Physics of Lipids* 132, pp. 225-234.
- Rangaiah G.P., 2001, Evaluation of genetic algorithms and simulated annealing for phase equilibrium and stability problems, *Fluid Phase Equilibria*, vol. 187-188, pp. 83-109.
- Rocha S.A., 2008, Cálculo do Equilíbrio de Fases Sólido-Líquido em Misturas binárias por meio de Técnicas de Minimização e Análise de Convexidade, *Dissertação de mestrado em Engenharia Química – FEQ – Unicamp*.
- Rocha S.A., Guirardello R., 2009, An approach to calculate solid–liquid phase equilibrium for binary mixtures, *Fluid Phase Equilibria* 281, pp. 12-21.
- Slaughter D.W.; Doherty M.F., 1995, Calculation of Solid-liquid Equilibrium and Crystallization Paths for Melt Crystallization Processes, *Chemical Engineering Science*, Vol. 50, Nº 11, pp. 1679-1694.
- Smith J.M., Van Ness H.C., Abbott M.M., 2004, *Introduction to Chemical Engineering Thermodynamics*, 7th ed., McGraw-Hill.